analytical chemistry

Article

Cite This: *Anal. Chem.* 2020, 92, 1363−1371

pubs.acs.org/ac

Solvent-Induced Protein Precipitation for Drug Target Discovery on the Proteomic Scale

Xiaolei Zhang,[†,‡] Qi Wang,[‡] Yanan Li,[‡] Chengfei Ruan,[‡] Shuyue Wang,[†,‡] Lianghai Hu,*[,†] and Mingliang Ye*[,‡]

[†]Key Laboratory for Molecular Enzymology & Engineering, the Ministry of Education, National Engineering Laboratory of AIDS Vaccine, School of Life Sciences, Jilin University, Changchun 130012, China

[‡]CAS Key Laboratory of Separation Sciences for Analytical Chemistry, National Chromatographic R&A Center, Dalian Institute of Chemical Physics, Chinese Academy of Sciences, Dalian 116023, China

Supporting Information

ABSTRACT: High-throughput drug discovery is highly dependent on the targets available to accelerate the process of candidates screening. Traditional chemical proteomics approaches for the screening of drug targets usually require the immobilization/modification of the drug molecules to pull down the interacting proteins. Recently, energetics-based proteomics methods provide an alternative way to study drug−protein interaction by using complex cell lysate directly without any modification of the drugs. In this study, we developed a novel energetics-based proteomics strategy, the solvent-induced protein precipitation (SIP) approach, to profile the interaction of drugs with their target proteins by using quantitative proteomics. The method is easy to use for any laboratory with the common chemical reagents of acetone, ethanol, and acetic acid. The SIP approach was able to identify the well-known protein targets of methotrexate, SNS-032, and a pan-kinase inhibitor of staurosporine in cell lysate. We further applied this approach to discover the off-targets of geldanamycin. Three known protein targets of the HSP90 family were successfully identified, and several potential off-targets including NADH dehydrogenase subunits NDUFV1 and NDUFAB1 were identified for the first time, and the NDUFV1 was validated by using Western blotting. In addition, this approach was capable of evaluating the affinity of the drug−target interaction. The data collectively proved that our approach provides a powerful platform for drug target discovery.

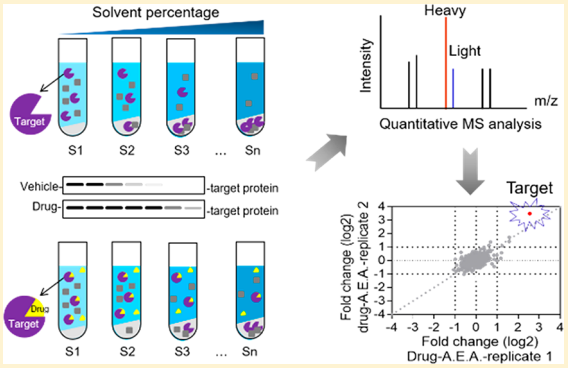

The systematic identification of drug target proteins plays a vital role in understanding the basic drug action mechanism.[1] A variety of chemical proteomics-based methods have been developed for the screening of drug targets. With the development of mass spectrometry-based proteomics, the affinity capture strategy, including activity-based probe profiling (ABPP) and affinity chromatography methods, has been used to explore the protein target landscape of a drug.[2−5] However, this conventional strategy typically requires the modification/immobilization of the small-molecule drug, which will usually alter specificity and/or affinity of small molecules[6] and therefore result in false positive identification of targets. Hence, it is highly desired to develop a strategy for the probing of drug−protein interactions with free drug without any modifications.

In recent years, several modification-free approaches have been developed for the study of drug−protein interactions,[7] e.g., drug affinity responsive target stability assay (DARTS),[8] stability of proteins from rates of oxidation (SPROX),[9,10] chemical denaturant and protein precipitation (CPP),[11] cellular thermal shift assay (CETSA), and thermal proteome profiling (TPP).[12−14] DARTS exploited the fact that proteins have higher resistance to proteolysis upon drug binding. The targets of FK506, rapamycin, and resveratrol were successfully identified by using this method.[15] In the SPROX approach, the target proteins are revealed by assessing the thermodynamic stability change of proteins upon ligand binding by measuring oxidation rates of methionine-containing residues as a function of the chemical denaturant concentration.[10] CPP was based on the principle of chemical denaturant induced proteins precipitation to identify the protein targets of drugs. As the emerging approaches in monitoring target engagement, CETSA and TPP reveal drug targets by measuring their resistance to heat-induced denaturation.[16] In CETSA, multiple aliquots of drug- or vehicle-treated cell lysate were heated to different temperatures to denature proteins. The proteins are gradually unfolded to expose the hydrophobic core with the increasing of temperature, resulting in the precipitation of the proteins in high temperature. The proteins that are stabilized by binding with drugs have higher resistance to the heat-

Received: October 4, 2019
Accepted: December 3, 2019
Published: December 3, 2019

DOI: 10.1021/acs.analchem.9b04531
Anal. Chem. 2020, 92, 1363−1371

induced precipitation. Thus, the change in the stability of the proteins could be measured by comparing the fractions of soluble proteins at high temperature between the drug-treated and vehicle-treated samples. In CETSA, the soluble proteins are separated by sodium dodecyl sulfate polyacrylamide gel electrophoresis (SDS−PAGE) and the potential proteins are quantified by Western blotting.[13] Although this method is a great tool to validate the drug targets, it is not applicable to discover unknown drug targets at the proteome-wide level. To circumvent this limitation, the TPP approach was developed for high-throughput identification of protein targets. Instead of using Western blotting as the readout, a quantitative proteomics approach was used to quantify proteins in soluble fractions, which allowed the discovery of ligand-induced stabilization of proteins at the proteome level.[17,18] This method was widely used to probe the interaction of small molecules with proteins in living cells, cell lysates, and even animal tissues.[17,19,20] Overall, the above approaches were all based on the principle that the proteins are stabilized after the binding of the drugs. The significant feature of these methods is that no modification of the drug is required.

Due to the ligand-induced stabilization, the ligand-binding protein targets are less sensitive to protease hydrolysis, oxidative denaturation, heat denaturation, and chemical denaturant. And therefore, corresponding methods (e.g., DARTS, SPROX, TPP, and CPP) are developed to screen drug targets. It is well-known that proteins could be denatured and precipitated by organic solvents,[21] and therefore, we hypothesized that this can be used for the probing of drug−protein interactions. Herein, we developed a novel method, the solvent-induced protein precipitation (SIP) approach, to identify the protein targets or off-targets of drugs, which was based on the concept that ligand-binding proteins were more tolerant to organic solvent. Organic solvent precipitates proteins by decreasing the dielectric constant and competing for protein hydration, which is different from thermal denaturation induced proteins precipitation. Some proteins such as BCR-ABL are not responsive to thermal denaturation after binding with dasatinib,[12] implying that the target space identified by different approaches may be complementary. Furthermore, chemical denaturation is more rigorous than temperature denaturation in a thermodynamic measurement. In addition, proteomic coverage yielded by the SIP approach is similar to that of the conventional bottom-up experiment, which is better than that produced by SPROX. The developed SIP approach was first evaluated with two model drugs of MTX and SNS-032 and successfully revealed the known targets. The ability of SIP to identify target binding was further validated by using the broad-specificity kinase inhibitor staurosporine, which induced stabilization shifts of many protein kinases. Last but not the least, geldanamycin was studied for the discovery of potential off-targets. Protein NDUFV1 was discovered as a potential off-target of geldanamycin and validated by using Western blotting. Additionally, the SIP approach could evaluate the affinity of the drug−target interaction, and the affinity of the novel target NDUFV1 of geldanmycin was estimated. We expect the extensive use of this approach in drug target discovery and mechanism studies in the future.

EXPERIMENTAL SECTION

Materials and Cell Culture. Dimethyl sulfoxide (DMSO), NP-40, protease inhibitor cocktail, formic acid (FA), dithiothreitol (DTT), iodoacetamide (IAA), and trypsin (bovine, TPCK-treated) were purchased from Sigma-Aldrich (St. Louis, MO, U.S.A.). Methotrexate (MTX) was purchased from Sigma-Aldrich; SNS-032, staurosporine, and geldanamycin were purchased from Selleck (Houston, TX); RPMI 1640 medium and phosphate-buffered saline (PBS, pH 7.4, 1×) were purchased from Gibco (Gaithersburg, MD). Acetonitrile and methanol (HPLC grade) were from Merck (Darmstadt, Germany). Pure water used in all experiments was purified with a Milli-Q system (Millipore, Milford, MA). The centrifugal filter unit was purchased from Sartorius. HeLa and 293T cells were cultured in RPMI 1640 containing 10% fetal bovine serum (FBS) (Gibco, New York) and 1% streptomycin (Beyond, Haimen, China) under the condition of 37 °C, 5% CO_2.

Preparation of Cell Extract for Stabilization Profiling. Cells were harvested and washed with cold PBS three times. Subsequently, cells were lysed using PBS containing 0.2% NP-40 at pH 7.4, and then supplemented with 1% EDTA-free cocktail. The cell suspensions were frozen using liquid nitrogen, followed by thawing at 37 °C using a water bath. When the cell suspensions were thawed about 60%, they were transferred on ice to continue thawing. This procedure was repeated three times. The soluble proteins in the supernatant were separated from cell debris by centrifuging at 20 000*g* for 10 min at 4 °C. The supernatant was divided into two aliquots; one aliquot was treated with a drug prepared in DMSO (the drug concentrations of MTX, SNS-032, staurosporine, and geldanamycin were 100, 100, 20, and 100 μM, respectively), and the other aliquot was treated with an equivalent amount DMSO alone as vehicle. After the incubation of the protein extract with the drug or vehicle for 20 min at room temperature using a rotometer at normal rotating speed, the extract was divided into seven aliquots of 100 μL in new 600 μL tubes. The denaturation was initiated by addition of an organic solvent mixture of acetone/ethanol/acetic acid (A.E.A.) with ratio of 50:50:0.1 to reach the final percentage of organic solvent ranging from 9% to 19%. Subsequently, the mixtures were equilibrated at 800 rpm for 20 min at 37 °C. Supernatants were collected after the mixtures were centrifuged at 20 000*g* for 10 min at 4 °C. One portion was used for Western blotting analysis, and the left portion was stored at −80 °C for the subsequent mass spectrometry (MS)-based quantification. The protein concentration was determined by a BCA protein assay kit (Thermo Fisher Scientific, San Jose, CA, U.S.A.).

Sample Preparation for MS Analysis. The above supernatants including the protein samples with or without ligands were processed with a filter-aided sample preparation (FASP) technique.[22] First, the equal volume of samples in the control group and drug-treated group were concentrated using a 10 k ultrafiltration tube (Sartorius AG, Germany) under the condition of 14 000*g* at 4 °C. The protein samples were washed two times with 8 M urea in the 50 mM HEPES, pH 8.0, the disulfide bonds were then reduced by addition of 20 mM DTT at 700 rpm for 2 h at 37 °C, followed by alkylation of the proteins by 40 mM IAA in dark at room temperature for 40 min. Subsequently, the protein samples were washed two times with 50 mM HEPES, and then trypsin was added to the samples at a ratio of 1:20 (enzyme/protein, w/w) for digestion at 37 °C for 16 h. The resulting peptides were then subjected to dimethyl labeling.[23] Subsequently, the two differentially labeled digests were mixed, and then subjected to desalting

DOI: 10.1021/acs.analchem.9b04531
Anal. Chem. 2020, 92, 1363−1371

with a C18 solid-phase extraction (Waters, Milford, MA) according to the manufacturer's protocol. Finally, the desalted samples were lyophilized in a SpeedVac (Thermo Fisher Scientific, San Jose, CA, U.S.A.) and stored at −80 °C before use.

Liquid Chromatography−Tandem Mass Spectrometry Analysis. The analysis of tryptic peptides was performed on an Ultimate 3000 RSLCnano system coupled with a Q-Exactive-HF mass spectrometer, controlled by Xcalibur software v2.1.0 (Thermo Fisher Scientific, Waltham, MA, U.S.A.). The dimethyl-labeled peptide samples were resolved in 0.1% formic acid/water and were quantified by using a NanoDrop 2000 (Thermo Fisher Scientific, U.S.A.). Briefly, 1 μg of the resuspended peptides was automatically loaded onto a C18 trap column (200 μm i.d.) at a flow rate of 5 μL/min. The capillary analytical column (150 μm i.d.) was packed in-house with 1.9 μm C18 ReproSil particles (Dr. Maisch GmbH). The mobile phases A and B were 0.1% FA and 80% ACN/0.1% FA, respectively. The flow rate was set as 600 nL/min. The gradient of the mobile phase was developed as follows: 9−13% mobile phase B for 1 min; 13−27% B for 79 min; 27−45% B for 17 min; 45−90% B for 1 min; 90% B was maintained for 10 min; and finally equilibration with mobile phase A for 12 min.

The liquid chromatography−tandem mass spectrometry (LC−MS/MS) system was operated in data-dependent MS/MS acquisition mode. The full mass scan acquired in the Orbitrap mass analyzer was from m/z 350 to 1750 with a resolution of 60 000 (m/z 200). The MS/MS scans were also acquired by the Orbitrap with a 15 000 resolution (m/z 200), and the AGC target was set to 5×10^4. The spray voltage and the temperature of the ion transfer capillary were set to 2.6 kV and 275 °C, respectively. The normalized collision energy for higher-energy collisional dissociation (HCD) and dynamic exclusion were set as 27% and 20 s, respectively.

Protein Identification and Quantification. Raw files were processed with MaxQuant (version 1.5.3.30.). The MS/MS spectra were searched against the Uniprot human database containing 70 037 entries (June 2018) with the Andromeda search engine in MaxQuant. Carbamidomethylated cysteine was searched as a fixed modification, whereas oxidation of methionine and N-terminal protein acetylation were searched as variable modifications. Multiplicity was set to 2; dimethLys0 and dimethNter0 were light labeling, whereas dimethLys4 and dimethNter4 were heavy labeling. Trypsin was set as the proteolytic enzyme, and up to two missed cleavages were allowed. Precursor and fragment mass tolerances were set at 10 ppm and 0.02 Da, respectively. The false discovery rate was set to 0.01 for both proteins and peptides. Moreover, the options of requantify and match between runs were required. Normalized H/L ratios were used for subsequent statistical analysis.

Data Processing. The data exported from MaxQuant was analyzed using Excel software. The normalized H/L ratio was presented as log2 fold change (FC) to generate a scatter plot based on LC−MS/MS data from two replicate runs. The proteins that were identified in both replicate runs were used for the subsequent analysis. The maximum average value was kept as the final log2 $FC_{(H/L\ normalization\ ratio)}$ if the protein target was identified in different samples. The proteins with average log2 $FC_{H/L\ normalization\ ratio)} > 1$ or < -1 in different samples of the same set of experiments were combined and considered as the total potential protein targets. The scatter plots were carried out by Graphpad Prism 7 software (Graphpad Software, Inc., La Jolla, CA).

Target Validation with Western Blotting. The soluble proteins in supernatants were separated by means of SDS−PAGE and were transferred onto a poly(vinylidene difluoride) (PVDF) membrane. The membrane was blocked with 5% skim milk. Primary anti-DHFR, anti-CDK9 (Subways, China), anti-HSP90AB1, anti-NDUFV1 (Proteintech, Chicago, IL), and anti-GAPDH (Abcam, Cambridge, U.K.) antibodies, secondary rabbit antimouse HRP-IgG, and goat antirabbit HRP-IgG antibodies (Abcam, Cambridge, U.K.) were used for immunoblotting. The chemiluminescence intensities were visualized and quantified by the ECL detection kit (Thermo Fisher Scientific, U.S.A.), and the images were obtained by using a Fusion FX7 imaging system (Vilber Infinit, France). The protein abundance was normalized by the protein intensity in the 9% A.E.A.-treated sample.

Affinity Evaluation with Dose-Dependent Response Assay. The affinity of the drug−target interaction was determined by dose-dependent response assay. The drug solutions with different concentrations (10^1, 10^0, 10^{-1}, 10^{-2}, 10^{-3}, 10^{-4}, 10^{-5}, 10^{-6}, 10^{-7}, 10^{-8}, 10^{-9} μM) were prepared by 10-fold diluting of geldanamycin stock solution of 10 μM. After HeLa cell lysates were treated with drug with different concentrations, each sample was treated with 15% A.E.A., followed by the procedure outlined above in the detailed information on sample preparation in cell lysate. The supernatants were analyzed by Western blotting, and the band intensity was plotted with Graphpad Prism software.

For validation of the novel protein target NDUFV1 of geldanamycin in dose-dependent response assay, the concentration of geldanamycin was starting at 100 μM and gradually diluted as a 10-fold dilution (10^2, 10^1, 10^0, 10^{-1}, 10^{-2}, 10^{-3}, 10^{-4}, 10^{-5}, 10^{-6}, 10^{-7}, 10^{-8} μM) following the procedure outlined above for the experiment on dose-dependent response.

Protein−Protein Interaction, Gene Ontology, and Pathways Analysis. The interaction of protein hits and gene ontology (GO) analysis was analyzed by using the online tool STRING (https://string-db.org/). The pathways analysis was conducted by using Reactome (http://reactome.org/). The clusters were arranged by Graphpad Prism 7 software.

RESULTS AND DISCUSSION

Establishment of the SIP Approach. Organic solvents such as acetone, ethanol, methanol, and acetonitrile are often used to precipitate proteins to remove contaminants. The precipitation is mainly attributed to two reasons, i.e., decrease in protein solubility resulting from reduction of the dielectric properties of the solution and destruction of the hydration membrane of the protein.[24] The ligand-binding protein complex has a lower energy state and therefore requires more energy to be unfolded than the free protein. Thus, in principle, the target proteins will become more resistant to the denaturation and precipitation induced by the treatment of organic solvent after the binding of the drugs. We hypothesized that the organic solvent induced protein precipitation can also be used to screen drug targets. In this study we explored a widely used organic solvent system (acetone/ethanol/acetic acid = 50:50:0.1, v/v/v, abbreviated as A.E.A.) to denature and precipitate proteins for the screening of drug targets. The workflow of this SIP approach is shown in Figure 1. Briefly, two aliquots of cell lysate were incubated with and without a

DOI: 10.1021/acs.analchem.9b04531
Anal. Chem. 2020, 92, 1363−1371

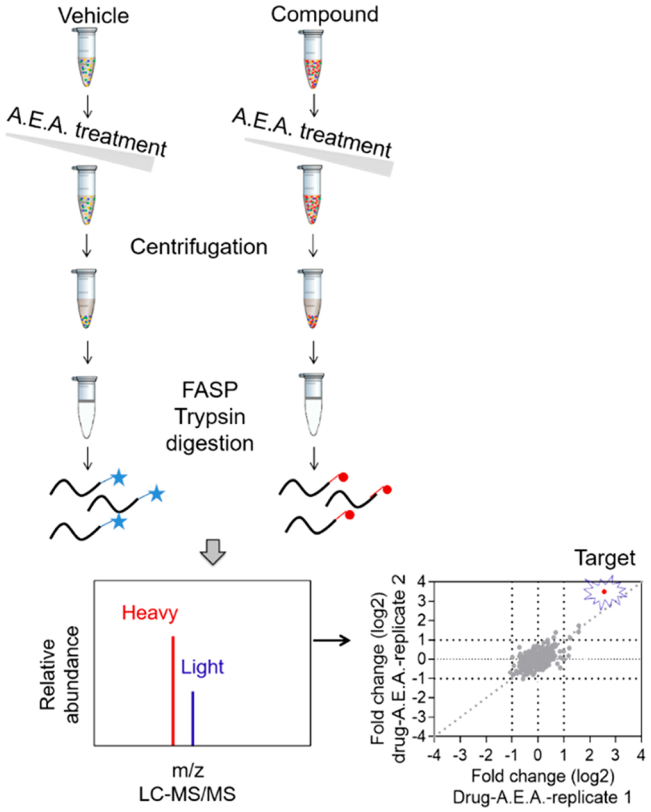

Figure 1. Schematic representation of the organic solvent induced protein precipitation (SIP) approach for the screening of drug targets. The cell lysate was incubated with or without drugs and treated with a particular percentage of organic solvent mixture (acetone/ethanol/acetic acid, A.E.A.) to precipitate proteins. After A.E.A. treatment, the soluble proteins were separated from precipitated proteins by centrifugation. The supernatants with/without drug treatment were subjected to a filter-aided sample preparation protocol and quantified by stable isotopic dimethyl labeling based proteomics. The proteins with consistently quantified change over 2 folds in two replicates are considered as the potential targets.

drug, respectively. Then, the same volume of organic solvent mixture A.E.A. was added to the two lysates to initiate protein precipitation. To demonstrate the stability difference with the binding of the drug in organic solvent, we explored a series of A.E.A. percentages from 9% to 19% for protein precipitation. After precipitation, the soluble proteins are separated from aggregated proteins by centrifugation. Theoretically, proteins will be more resistant to precipitation at a certain percentage of solvent when they bind to drugs. Therefore, potential drug affinity proteins will be determined by quantitative proteome analysis of the supernatants of cell lysates after precipitation. In this workflow, the two protein samples with/without the drug were collected for comparative proteome analysis after protein digestion and stable isotope dimethyl labeling. All the samples were analyzed by LC−MS/MS replicate, and only the proteins quantified in both runs were used for further analysis. The average log2 $FC_{(H/L\ normalization\ ratio)}$ > 1 or < −1 was considered as the potential protein targets.

Validation of the Approach by Model Drugs. Methotrexate, a well-characterized model drug, was used to evaluate the feasibility of this method. MTX is an anti-folate drug which selectively inhibits dihydrofolate reductase (DHFR) to prevent the synthesis of tetrahydrofolic acid and thus causes the death of cancer cells.[20] In this study, 293T cell lysate was incubated with 100 μM MTX for 20 min at room temperature, and was then treated with different percentages of organic solvent mixture A.E.A. After the removal of precipitates, we quantified the abundance of protein target DHFR in the supernatant by Western blotting. As shown in Figure 2A, the DHFR signal in the control lysate started to decrease at 11% A.E.A. and almost completely disappeared at 15%, which indicated that the DHFR protein completely precipitated at this solvent concentration. However, the signal of DHFR for MTX-incubated cell lysate barely decreased at a much higher solvent percentage of 17% A.E.A. The Western blotting-based curve of DHFR protein abundance exhibited significant stabilization shifts in the presence of MTX (Figure 2A). Next, the samples treated with 13% and 15% A.E.A. in the control and drug-treated groups were subjected to FASP and dimethyl labeling for quantitative proteomics. Through mass spectrometry analysis, DHFR was identified in the two labeled samples, and the maximum average log2 $FC_{(H/L\ normalization\ ratio)}$ nearly reached 4, indicating significant stabilization after the binding of the drug. This proteomics readout was well-consistent with the result of Western blotting (Figure 2, parts B and C). We explored our approach to another example of SNS-032, which was designed as an inhibitor of cyclin protein to prevent the proliferation of tumor cells.[25] As we expected, after treatment with 11% and 12% A.E.A., the Western blotting-based curve of CDK9 protein abundance exhibited significant stabilization shifts in the presence of SNS-032 (Figure 2D). Subsequently, the two labeled samples treated with 12% and 13% A.E.A. in the control and drug-treated groups were subjected to dimethyl labeling and quantitative proteomics analysis. Two known targets CDK2 and GSK-3α toward drug SNS-032 were identified (Figure 2, parts E and F). Moreover, the average log2 $FC_{(H/L\ normalization\ ratio)}$ of CDK2 and GSK-3α were 1.23 and 1.13, respectively (Figure 2, parts E and F), indicating the drug binding induced protein stabilization. The above data confirmed that the SIP approach was able to identify drug targets with high specificity.

Application of the Approach to a Pan-Kinase Inhibitor. The SIP approach was further extended to the screening of the targets of the broad-specificity kinase inhibitor staurosporine. The 293T cell extracts treated with staurosporine or vehicle were subjected to organic solvent induced protein precipitation with 15%, 16%, and 17% A.E.A., and the resulting supernatants were analyzed by the above-mentioned proteomic workflow in two runs. Overall, 1752, 1648, and 1566 proteins were quantified in the three A.E.A.-treated samples in the staurosporine experiment. Though over 1500 proteins were quantified in each experiment, only a few proteins were found to have significant changes after the binding of the drug. In total, 12, 9, and 5 proteins displayed stabilization shifts that passed our significance criteria in the three samples, and seven, five, and four protein kinases were identified among them (Figure S1A−C). It was found that STK4 kinase was the most consistently observed hit and was identified in all the three different percentages of A.E.A.-treated samples. Several kinases such as SIK, KCC2D, STK10, and PHKG2 were identified twice among the three samples. Bringing the protein kinase targets identified in the three samples together, totally nine kinases were identified as target proteins for staurosporine (Table S1). In addition, we also observed 11 non-kinase proteins stabilized after the binding of drug (Table S1). This indicated that non-kinase proteins could

DOI: 10.1021/acs.analchem.9b04531
Anal. Chem. 2020, 92, 1363−1371

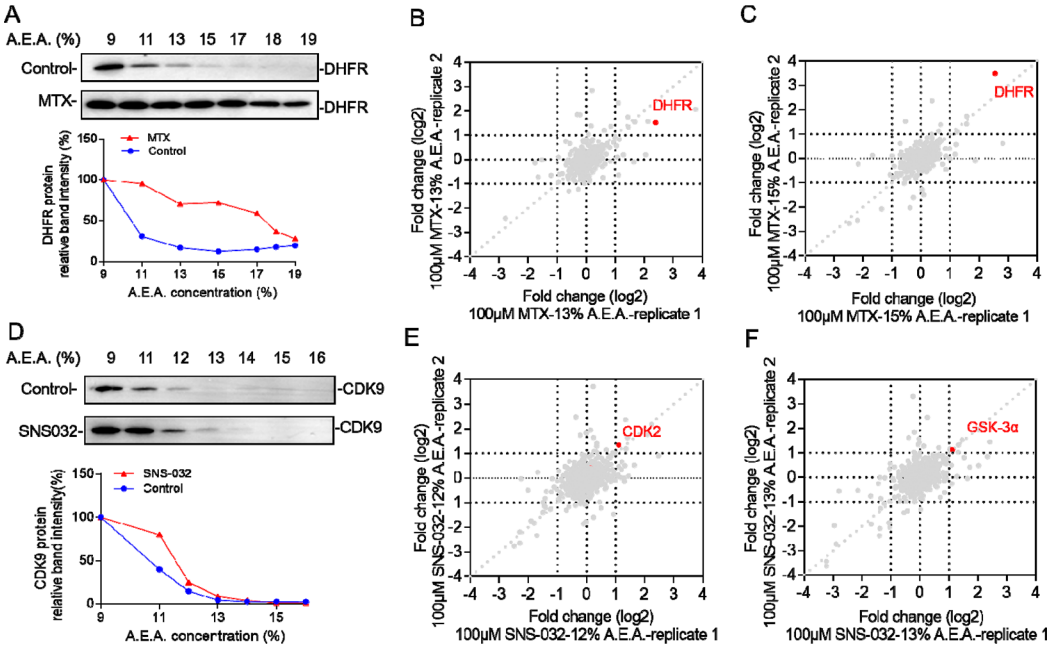

Figure 2. SIP approach to identify the known targets of MTX and SNS-032. (A) Western blotting confirming the stabilization of DHFR by MTX in 293T cell lysate. The relative band intensity was normalized by the protein intensity in the 9% A.E.A.-treated sample. Scatter plot of fold change of DHFR protein abundance in (B) 13% and (C) 15% A.E.A.-treated samples. The target hits were obtained by LC−MS/MS data from two replicate runs. (D) Western blotting confirming the stabilization of CDK9 by SNS-032 in 293T cell lysate. The relative band intensity was normalized by the protein intensity in the 9% A.E.A.-treated sample. Scatter plot of fold change of CDK9 protein abundance in (E) 12% and (F) 13% A.E.A.-treated samples. The target hits were obtained by LC−MS/MS data from two replicate runs.

be the target proteins of kinase inhibitors, which was also reported in previous studies.[12]

Savitski et al. have performed a comprehensive study to screen the targets of staurosporine by the TPP approach.[12] In their study, the samples from 10 different temperatures were labeled with the neutron-encoded isobaric mass tagging reagents (TMT10) and analyzed with two-dimensional reversed-phase liquid chromatography−tandem mass spectrometry (2D RP-RPLC−MS/MS), which resulted in the quantification of 7677 proteins (Figure S2A). In total, the thermal profiles comprised 260 protein kinases, of which 51 (19.62%) were determined to be the target proteins according to the melting curves (Figure S2B), while in this study, the samples from three different solvent concentrations were separately subjected to dimethyl labeling and 1D RPLC−MS/MS analysis, which quantified only 1854 proteins (Figure S2A). Due to the poor proteome coverage, only 19 protein kinases were quantified in this study. Among them, 47.37% (9/19) were found to be significantly stabilized after binding of the drug and determined to be the potential target proteins (Figure S2B). The comparison of the quantified kinases and the determined protein kinase targets between SIP and TPP is given in Figure S2. Because of the high proteome coverage of the TPP studies, 15 protein kinases quantified in this study were included in the 260 protein kinases (Figure S2B). As these 15 protein kinases were quantified in both studies, it is of interest to see if they showed a stabilization shift in both cases. It was found that only five protein kinases had significant stabilization shifts in both TPP and SIP (Figure S2C). There were four protein kinases including SIK, KCC2D, STK10, and KKCC1 that showed significant stabilization only in the SIP approach but not in the TPP approach, and no protein was found to have significant stabilization shift only in the TPP approach (Figure S2C). The comparison would be fairer if the proteome coverage for SIP was equivalent to that of TPP. However, the above data already indicated that target proteins identified by the different precipitation approaches are complementary.

Discovery of Off-Targets for Geldanamycin. Geldanamycin is the pioneering and potent inhibitor of HSP90 by binding to the unique ATP/ADP binding domain of HSP90.[26,27] However, it was withdrawn from clinical trials due to the serious side effects which lead to severe hepatotoxicity.[28] Therefore, SIP was applied to construct the target space of geldanamycin, which should reveal the intended on-targets and the unexpected off-targets.

By using Western blotting, we investigated the effect of different A.E.A. percentages on the precipitation of a known target protein HSP90AB1 of geldanamycin with and without the presence of geldanamycin in the total cell lysate of HeLa cells. It can be seen from Figure 3A that HSP90AB1 started to precipitate when the A.E.A. percentage increased from 15% to 17%. And it was obvious that the HSP90AB1 in the drug-treated sample was more resistant to organic solvent induced precipitation (Figure 3A), indicating the target protein was stabilized by geldanamycin. On the basis of the above investigation, samples treated with 15%, 16%, and 17% A.E.A. were subjected to dimethyl labeling for MS analysis at the proteome level, as obvious precipitation was observed for these samples.

After quantitative proteomics analysis, 1670, 1594, and 1405 proteins were quantified in the three A.E.A.-treated samples of geldanmycin experiment (Figure S3), respectively. Among them, 53 protein hits with average log2 $FC_{(H/L\ normalization\ ratio)} > 1$ and 33 protein hits with average log2 $FC_{(H/L\ normalization\ ratio)} < -1$ were discovered, and they were considered as direct and indirect candidate targets of geldanamycin. These hits were ranked by average log2 $FC_{(H/L\ normalization\ ratio)}$ values (Tables S2

DOI: 10.1021/acs.analchem.9b04531
Anal. Chem. 2020, 92, 1363−1371

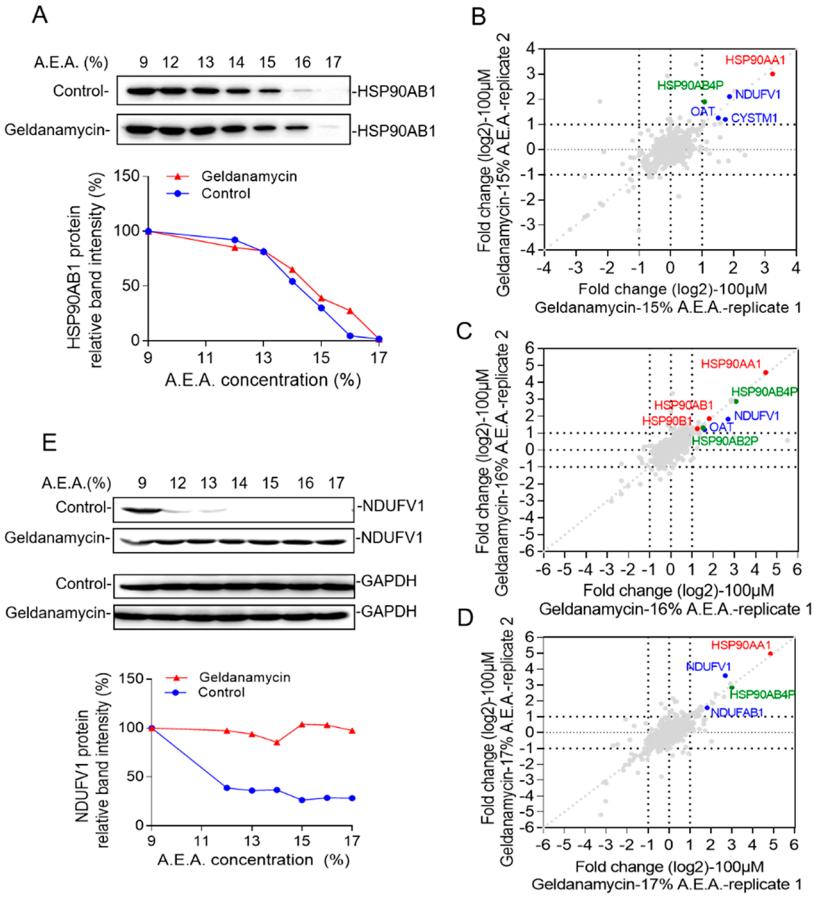

Figure 3. Discovery of protein targets of geldanamycin by the SIP approach and validation of screened potential off-target protein NDUVF1 through the Western blotting technique. (A) Western blotting confirming the stabilization of geldanamycin by HSP90AB1 in HeLa cell lysate. The relative band intensity was normalized by the protein intensity in the 9% A.E.A.-treated sample. Scatter plot of fold change of HSP90AB1 protein abundance in (B) 15%, (C) 16%, and (D) 17% A.E.A.-treated samples. The target hits were obtained by LC−MS/MS data from two replicate runs. The red dots represent the well-known protein target HSP90 family (HSP90AB1, HSP90AA1, and HSP90B1) of geldanamycin. The green dots represent the novel HSP90 isoforms proteins. Blue dots represent potential candidate targets. (E) Western blotting confirming the stabilization of geldanamycin by NDUFV1 protein in HeLa cell lysate. The relative band intensity was normalized by the protein intensity in the 9% A.E.A.-treated sample.

and S3). In fact, it is arbitrary to define the criterion for screening target proteins as log2 FC. Loosening filtering criteria is able to improve the sensitivity of target proteins identification, but also has the risk to increase false positive identifications.

As expected, the three known protein targets of geldanamycin, HSP90AA1, HSP90AB1, and HSP90B1, were successfully identified, and the maximum average log2 $FC_{(H/L\ normalization\ ratio)}$ values were 4.90, 2.83, and 1.25 (Table S2), indicating significant stabilization was yielded after binding of geldanamycin. HSP90AA1 was reproducibly identified among these three samples with different A.E.A. percentages (Figure 3B−D). Furthermore, the other HSP90 isoforms such as HSP90AB2P and HSP90AB4P were also reproducibly identified, and the maximum average log2 $FC_{(H/L\ normalization\ ratio)}$ values were 1.41 and 2.97, respectively (Table S2).

All stabilized and destabilized protein hits excluding the known HSP90 family proteins were subjected to gene ontology and pathways analysis. It was found that most of the protein hits were involved in metabolism, oxidation−reduction processes, and mitochondria function (Figure S4A−D). Our result was consistent with the previous study demonstrating reactive oxygen species mediate geldanamycin-induced hepatotoxicity by phenotypic analysis.[29] The above data collectively demonstrated that the hepatotoxicity induced by geldanamycin may be due to the promiscuous off-target effects (Figure S4E). The identification of these target proteins indicated the high reliability of this approach to construct the target space.

It was worth noting that protein NDUFV1 was the top candidate target and repeatedly identified in all the three different percentages of A.E.A.-treated samples (Figure 3B−D). NDUFV1 is the core subunit of the mitochondrial membrane respiratory chain NADH dehydrogenase, which was also known as Complex I,[30] and the other subunit NDUFAB1 of mitochondrial Complex I was also found to be stabilized (Figure 3D). We further used Western blotting to confirm whether NDUFV1 was stabilized after incubation with geldanamycin. The Western blotting detection of soluble proteins illustrated that the abundance of NDUFV1 protein without geldanamycin decreased significantly at 12% A.E.A. (Figure 3E), while its abundance with geldanamycin kept constant even with the highest percentage of A.E.A. (17%). The Western blotting-based curve of NDUFV1 protein abundance exhibited significant stabilization shifts in the

DOI: 10.1021/acs.analchem.9b04531
Anal. Chem. 2020, 92, 1363−1371

presence of geldanamycin (Figure 3E). Both the quantitative proteomics and Western blotting readout indicated NDUFV1 was strongly stabilized after binding with geldanamycin, and therefore NDUFV1 is a high-confidence off-target of geldanamycin.

Savitski et al.[12] reported that the affinity data obtained by dose-dependent response in TPP were in good agreement with data from kinobeads competition-binding experiments. Therefore, we exploited dose-dependent response assay to determine the affinity of geldanamycin with the well-known protein target HSP90AB1. The HeLa cell lysate was exposed to different concentrations of geldanamycin, and then treated with a defined 15% A.E.A. The detection of the curve fitted by Western blotting showed the abundance of HSP90AB1 obviously decreased from the concentration at 1 μM (Figure 4A). The half-saturation point of the geldanamycin-binding

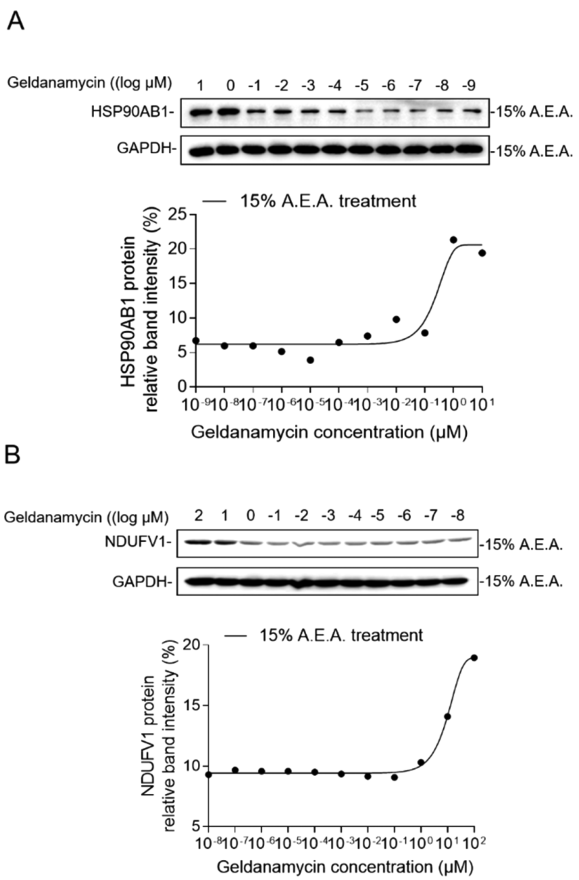

Figure 4. Evaluating affinity for ligand–protein interaction through using the SIP approach. (A) Affinity between geldanamycin and target protein HSP90AB1 was estimated in HeLa lysate after incubating with different concentrations of the drug geldanamycin at fixed A.E.A. concentration by using Western blotting. (B) Measuring the affinity between geldanamycin and protein NDUFV1 in HeLa lysate after incubating with different concentrations of the drug geldanamycin at fixed A.E.A. concentration by using Western blotting.

HSP90AB1 complex was between 0.1 and 1 μM concentration, and geldanamycin reached the full occupancy of HSP90AB1 protein around the concentration of 1 μM (Figure 4A). The affinity of the drug geldanamycin evaluated by the SIP approach was roughly consistent with previously reported K_d values (1.2 μM). This is not surprising as the stabilization shift depends on the fraction of proteins binding to the drug, which depends on K_d values. Clearly, the SIP approach is also able to determine the affinity of the drug–protein interaction. Conventional methods, e.g., isothermal titration calorimetry (ITC),[31,32] require the use of purified protein, which is time-consuming, and for some cases the purified protein is not available. However, SIP enables the determination of the affinity of a drug with a protein target only using cell lysate when Western blotting readout was applied. If antibody is not available, quantitative proteomics coupled with dose-dependent response assay could also be applied to determine the affinity of a drug with its targets. This technique is more powerful as it can determine the affinity of a drug with multiple protein targets.

To assess the affinity of geldanamycin for its novel target NDUFV1, drug dose-dependent response assay at a fixed A.E.A. percentage of 15% was performed. The Western blotting-based curve confirmed that the half-saturation point of the latent target protein NDUFV1 of geldanamycin was around 10 μM, and geldanamycin reached the full occupancy at 100 μM, which was about 10 times higher than that in the interaction between geldanamycin and its known HSP90AB1 proteins (Figure 4B). This result implied that NDUFV1 protein was captured as off-target-induced side effects once the drug geldanamycin dosage increased, which was well in agreement with the study that dose-limiting hepatotoxicity of geldanamycin is due to the quinine moiety.[33]

Analysis of the Proteins Destabilized by Geldanamycin. We are also interested in the proteins with the reduction of stability with the addition of ligand to the cell lysate. Ahsan et. al reported that inhibitors of protein–protein interaction could cause protein destabilization.[34] Savitski et al. reported that inhibition by staurosporine (ligand) stabilizes the catalytic subunit (target) but destabilizes the regulatory subunit, which indicated that staurosporine occupies the binding sites of the catalytic subunit, resulting in the dissociation of the regulatory subunit.[12] HSP90 inhibitors target the ATP-binding domain, leading to the dissociation of weak client proteins of HSP90.[35,36] Therefore, the destabilized proteins in this study were possibly caused by the effect of inhibiting protein–protein interactions of geldanamycin, which resulted in client proteins of HSP90 or other protein subunits dissociated from the protein complexes. The analysis of protein–protein interactions toward all protein hits confirmed the above assumption. It was found that there were many interactions between the stabilized proteins and destabilized proteins (Figure S5A). Among these 33 destabilized proteins, 22 interacted with stabilized proteins (destabilized protein–stabilized protein interaction, DSI) in some way, and the percentage was 60.60% (Figure S5B). The high percentage of DSI further indicated these proteins were likely dissociated from the protein complex due to the binding of the drug with a direct target protein in the protein complex.

CONCLUSION

In this study we presented a novel energetics-based approach to screen drug targets. It relies on the fact that the ligand binding proteins have higher resistance to solvent-induced precipitation (SIP). By combining with quantitative proteomics, this SIP approach enables the discovery of drug targets in the total cell lysate without modification of the drug. This approach was applied to screen the target proteins of three model drugs of MTX, SNS-032, and staurosporine. The known targets were identified as top hits indicating the effectiveness of

DOI: 10.1021/acs.analchem.9b04531
Anal. Chem. 2020, 92, 1363–1371

this approach. This approach was further applied to explore the target space of geldanamycin, and 53 proteins directly binding with drug were screened. Furthermore, the candidate off-target NDUFV1 was validated by using Western blotting. This approach can also determine the drug−protein affinity in total cell lysate using dose−response assay. As an example, the affinity of the novel target NDUFV1 of geldanamycin was determined. Taken together, the SIP approach provides a good platform for drug target identification so as to better understand the side effects and the mechanism of action.

■ ASSOCIATED CONTENT

Supporting Information

The Supporting Information is available free of charge at https://pubs.acs.org/doi/10.1021/acs.analchem.9b04531.

SIP approach to identify the kinase targets of the broad-specificity inhibitor staurosporine, comparison between SIP and TPP on protein kinases directly binding with staurosporine, Venn diagram showing the protein coverage of the geldanamycin experiment, GO analysis of candidate protein targets of geldanamycin identified by the SIP approach, potential mechanism of geldanamycin-induced hepatotoxicity, the association between stabilized proteins and destabilized protein, the proteins stabilized due to the presence of staurosporine and geldanamycin, and the proteins destabilized due to the presence of geldanamycin (PDF)

■ AUTHOR INFORMATION

Corresponding Authors

*E-mail: lianghaihu@jlu.edu.cn.
*E-mail: mingliang@dicp.ac.cn.

ORCID

Xiaolei Zhang: 0000-0002-2372-2706
Shuyue Wang: 0000-0001-7470-0999
Lianghai Hu: 0000-0002-1246-6524
Mingliang Ye: 0000-0002-5872-9326

Notes

The authors declare no competing financial interest.

■ ACKNOWLEDGMENTS

This work was supported, in part, by funds from the China State Key Basic Research Program Grants (2016YFA0501402, 2017YFA0505004), the National Natural Science Foundation of China (21675061, 21535008, 91753105), the LiaoNing Revitalization Talents Program, and the innovation program (DICP TMSR201601, DICP&QIBEBT UN201802 and DICP I201935) of science and research from the DICP, CAS. M.Y. is a recipient of the National Science Fund of China for Distinguished Young Scholars (21525524).

■ REFERENCES

(1) Bantscheff, M.; Eberhard, D.; Abraham, Y.; Bastuck, S.; Boesche, M.; Hobson, S.; Mathieson, T.; Perrin, J.; Raida, M.; Rau, C.; Reader, V.; Sweetman, G.; Bauer, A.; Bouwmeester, T.; Hopf, C.; Kruse, U.; Neubauer, G.; Ramsden, N.; Rick, J.; Kuster, B.; Drewes, G. *Nat. Biotechnol.* **2007**, *25*, 1035−1044.

(2) Lentz, C. S.; Sheldon, J. R.; Crawford, L. A.; Cooper, R.; Garland, M.; Amieva, M. R.; Weerapana, E.; Skaar, E. P.; Bogyo, M. *Nat. Chem. Biol.* **2018**, *14*, 609−617.

(3) van Esbroeck, A. C. M.; Janssen, A. P. A.; Cognetta, A. B.; Ogasawara, D.; Shpak, G.; van der Kroeg, M.; Kantae, V.; Baggelaar, M. P.; de Vrij, F. M. S.; Deng, H.; Allara, M.; Fezza, F.; Lin, Z.; van der Wel, T.; Soethoudt, M.; Mock, E. D.; den Dulk, H.; Baak, I. L.; Florea, B. I.; Hendriks, G.; de Petrocellis, L.; Overkleeft, H. S.; Hankemeier, T.; De Zeeuw, C. I.; Di Marzo, V.; Maccarrone, M.; Cravatt, B. F.; Kushner, S. A.; van der Stelt, M. *Science* **2017**, *356*, 1084−1087.

(4) Dai, J. Y.; Liang, K.; Zhao, S.; Jia, W. T.; Liu, Y.; Wu, H. K.; Lv, J.; Cao, C.; Chen, T.; Zhuang, S. T.; Hou, X. M.; Zhou, S. J.; Zhang, X. N.; Chen, X. W.; Huang, Y. Y.; Xiao, R. P.; Wang, Y. L.; Luo, T. P.; Xiao, J. Y.; Wang, C. *Proc. Natl. Acad. Sci. U. S. A.* **2018**, *115*, E5896−E5905.

(5) Hoehenwarter, W.; Thomas, M.; Nukarinen, E.; Egelhofer, V.; Rohrig, H.; Weckwerth, W.; Conrath, U.; Beckers, G. J. M. *Mol. Cell. Proteomics* **2013**, *12*, 369−380.

(6) Nomura, D. K.; Dix, M. M.; Cravatt, B. F. *Nat. Rev. Cancer* **2010**, *10*, 630−638.

(7) Lyu, J. w.; Wang, K. Y.; Ye, M. L. *TrAC, Trends Anal. Chem.* **2019**, in press.

(8) Chin, R. M.; Fu, X. D.; Pai, M. Y.; Vergnes, L.; Hwang, H.; Deng, G.; Diep, S.; Lomenick, B.; Meli, V. S.; Monsalve, G. C.; Hu, E.; Whelan, S. A.; Wang, J. X.; Jung, G.; Solis, G. M.; Fazlollahi, F.; Kaweeteerawat, C.; Quach, A.; Nili, M.; Krall, A. S.; Godwin, H. A.; Chang, H. R.; Faull, K. F.; Guo, F.; Jiang, M. S.; Trauger, S. A.; Saghatelian, A.; Braas, D.; Christofk, H. R.; Clarke, C. F.; Teitell, M. A.; Petrascheck, M.; Reue, K.; Jung, M. E.; Frand, A. R.; Huang, J. *Nature* **2014**, *510*, 397−401.

(9) West, G. M.; Tucker, C. L.; Xu, T.; Park, S. K.; Han, X. M.; Yates, J. R.; Fitzgerald, M. C. *Proc. Natl. Acad. Sci. U. S. A.* **2010**, *107*, 9078−9082.

(10) Strickland, E. C.; Geer, M. A.; Tran, D. T.; Adhikari, J.; West, G. M.; DeArmond, P. D.; Xu, Y.; Fitzgerald, M. C. *Nat. Protoc.* **2013**, *8*, 148−161.

(11) Meng, H.; Ma, R. Z.; Fitzgerald, M. C. *Anal. Chem.* **2018**, *90*, 9249−9255.

(12) Savitski, M. M.; Reinhard, F. B.; Franken, H.; Werner, T.; Savitski, M. F.; Eberhard, D.; Molina, D. M.; Jafari, R.; Dovega, R. B.; Klaeger, S.; Kuster, B.; Nordlund, P.; Bantscheff, M.; Drewes, G. *Science* **2014**, *346*, 1255784.

(13) Molina, D. M.; Jafari, R.; Ignatushchenko, M.; Seki, T.; Larsson, E. A.; Dan, C.; Sreekumar, L.; Cao, Y.; Nordlund, P. *Science* **2013**, *341*, 84−7.

(14) Franken, H.; Mathieson, T.; Childs, D.; Sweetman, G. M. A.; Werner, T.; Togel, I.; Doce, C.; Gade, S.; Bantscheff, M.; Drewes, G.; Reinhard, F. B. M.; Huber, W.; Savitski, M. M. *Nat. Protoc.* **2015**, *10*, 1567−1593.

(15) Lomenick, B.; Hao, R.; Jonai, N.; Chin, R. M.; Aghajan, M.; Warburton, S.; Wang, J. N.; Wu, R. P.; Gomez, F.; Loo, J. A.; Wohlschlegel, J. A.; Vondriska, T. M.; Pelletier, J.; Herschman, H. R.; Clardy, J.; Clarke, C. F.; Huang, J. *Proc. Natl. Acad. Sci. U. S. A.* **2009**, *106*, 21984−21989.

(16) Almqvist, H.; Axelsson, H.; Jafari, R.; Dan, C.; Mateus, A.; Haraldsson, M.; Larsson, A.; Molina, D. M.; Artursson, P.; Lundback, T.; Nordlund, P. *Nat. Commun.* **2016**, *7*, 11040.

(17) Becher, I.; Andres-Pons, A.; Romanov, N.; Stein, F.; Schramm, M.; Baudin, F.; Helm, D.; Kurzawa, N.; Mateus, A.; Mackmull, M. T.; Typas, A.; Muller, C. W.; Bork, P.; Beck, M.; Savitski, M. M. *Cell* **2018**, *173*, 1495−1507.

(18) Savitski, M. M.; Zinn, N.; Faelth-Savitski, M.; Poeckel, D.; Gade, S.; Becher, I.; Muelbaier, M.; Wagner, A. J.; Strohmer, K.; Werner, T.; Melchert, S.; Petretich, M.; Rutkowska, A.; Vappiani, J.; Franken, H.; Steidel, M.; Sweetman, G. M.; Gilan, O.; Lam, E. Y. N.; Dawson, M. A.; Prinjha, R. K.; Grandi, P.; Bergamini, G.; Bantscheff, M. *Cell* **2018**, *173*, 260−274.

(19) Becher, I.; Werner, T.; Doce, C.; Zaal, E. A.; Togel, I.; Khan, C. A.; Rueger, A.; Muelbaier, M.; Salzer, E.; Berkers, C. R.; Fitzpatrick, P. F.; Bantscheff, M.; Savitski, M. M. *Nat. Chem. Biol.* **2016**, *12*, 908−910.

DOI: 10.1021/acs.analchem.9b04531
Anal. Chem. 2020, 92, 1363−1371

(20) Huber, K. V. M.; Olek, K. M.; Muller, A. C.; Tan, C. S. H.; Bennett, K. L.; Colinge, J.; Superti-Furga, G. *Nat. Methods* **2015**, *12*, 1055−1057.
(21) Cham, B. E.; Knowles, B. R. *J. Lipid Res.* **1976**, *17*, 176−181.
(22) Wisniewski, J. R. *Anal. Chem.* **2016**, *88*, 5438−5443.
(23) Boersema, P. J.; Raijmakers, R.; Lemeer, S.; Mohammed, S.; Heck, A. J. R. *Nat. Protoc.* **2009**, *4*, 484−494.
(24) Cowan, D. A. *Comp Biochem Phys. A* **1997**, *118*, 429−438.
(25) Olson, C. M.; Jiang, B. S.; Erb, M. A.; Liang, Y. K.; Doctor, Z. M.; Zhang, Z. N.; Zhang, T. H.; Kwiatkowski, N.; Boukhali, M.; Green, J. L.; Haas, W.; Nomanbhoy, T.; Fischer, E. S.; Young, R. A.; Bradner, J. E.; Winter, G. E.; Gray, N. S. *Nat. Chem. Biol.* **2018**, *14*, 163−170.
(26) Kamal, A.; Thao, L.; Sensintaffar, J.; Zhang, L.; Boehm, M. F.; Fritz, L. C.; Burrows, F. J. *Nature* **2003**, *425*, 407−410.
(27) Trepel, J.; Mollapour, M.; Giaccone, G.; Neckers, L. *Nat. Rev. Cancer* **2010**, *10*, 537−549.
(28) Ochel, H. J.; Eichhorn, K.; Gademann, G. *Cell Stress Chaperones* **2001**, *6*, 105.
(29) Samuni, Y.; Ishii, H.; Hyodo, F.; Samuni, U.; Krishna, M. C.; Goldstein, S.; Mitchell, J. B. *Free Radical Biol. Med.* **2010**, *48*, 1559−1563.
(30) Vinothkumar, K. R.; Zhu, J.; Hirst, J. *Nature* **2014**, *515*, 80−84.
(31) Brautigam, C. A.; Zhao, H. Y.; Vargas, C.; Keller, S.; Schuck, P. *Nat. Protoc.* **2016**, *11*, 882−894.
(32) Keller, S.; Vargas, C.; Zhao, H. Y.; Piszczek, G.; Brautigam, C. A.; Schuck, P. *Anal. Chem.* **2012**, *84*, 5066−5073.
(33) Samuni, Y.; Ishii, H.; Hyodo, F.; Samuni, U.; Krishna, M. C.; Goldstein, S.; Mitchell, J. B. *Free Radical Biol. Med.* **2010**, *48*, 1559−63.
(34) Ahsan, A.; Ray, D.; Ramanand, S. G.; Hegde, A.; Whitehead, C.; Rehemtulla, A.; Morishima, Y.; Pratt, W. B.; Osawa, Y.; Lawrence, T. S.; Nyati, M. K. *J. Biol. Chem.* **2013**, *288*, 26879−86.
(35) Schneider, C.; SeppLorenzino, L.; Nimmesgern, E.; Ouerfelli, O.; Danishefsky, S.; Rosen, N.; Hartl, F. U. *Proc. Natl. Acad. Sci. U. S. A.* **1996**, *93*, 14536−14541.
(36) Taipale, M.; Krykbaeva, I.; Koeva, M.; Kayatekin, C.; Westover, K. D.; Karras, G. I.; Lindquist, S. *Cell* **2012**, *150*, 987−1001.

DOI: 10.1021/acs.analchem.9b04531
Anal. Chem. 2020, 92, 1363−1371